Journal of Molecular Graphics and Modelling 34 (2012) 1–9

Contents lists available at SciVerse ScienceDirect

Journal of Molecular Graphics and Modelling

journal homepage: www.elsevier.com/locate/JMGM

Theoretical design and screening of panchromatic phthalocyanine sensitizers derived from TT1 for dye-sensitized solar cells

Linlin Yang[a], Lianshun Guo[a], Qianqian Chen[a], Huafei Sun[a], Jie Liu[a], Xianxi Zhang[a,*], Xu Pan[b,**], Songyuan Dai[b]

[a] Shandong Provincial Key Laboratory of Chemical Energy Storage and Novel Cell Technology, School of Chemistry and Chemical Engineering, Liaocheng University, Liaocheng 252059, China
[b] Division of Solar Energy Materials and Engineering, Institute of Plasma Physics, Chinese Academy of Sciences, P.O. Box 1126, Hefei, Anhui 230031, China

ARTICLE INFO

Article history:
Received 26 September 2011
Received in revised form 2 December 2011
Accepted 3 December 2011
Available online 13 December 2011

Keywords:
Dye-sensitized solar cells
DFT calculations
Molecule design
Orbital energy level
Electronic absorption spectra
Phthalocyanine

ABSTRACT

Computational screening of new dyes is becoming an extremely powerful tool, especially when associated with experimental synthetic efforts that might eventually lead to new and more efficient products. Nine novel unsymmetrical zinc phthalocyanine complexes derived from TT1 were designed as sensitizer candidates for dye-sensitized solar cells with three peripheral —CH_3, —OH, —OCH_3, —OPh, —NH_2, —$NHCH_3$, —$N(CH_3)_2$, —NHPh and —$N(Ph)_2$ substituents as the donors and a carboxyl group as the acceptor. The molecular orbital and the electronic absorption spectra properties of these compounds were studied and compared to those of TT1 using the density functional theory and time-dependent density functional theory calculations at B3LYP level with the LANL2DZ basis set. The novel candidates bearing the —NH_2, —$NHCH_3$, —$N(CH_3)_2$, —NHPh and —$N(Ph)_2$ moieties as the donors were found to be very promising for providing higher efficiencies than that of TT1 or even the current 4.6% efficiency record held by PcS6. They have higher LUMO levels, smaller energy gaps and red-shifted absorption bands compared to those of TT1. The new absorption bands emerging in 450–600 nm regions may promote ZnPcL—NH_2, ZnPcL—$NHCH_3$, ZnPcL—$N(CH_3)_2$, ZnPcL—NHPh and ZnPcL—$N(Ph)_2$ from near infrared to panchromatic sensitizers. Further experimental synthetic efforts are in progress in our group to validate the predictions in this report.

1. Introduction

Dye-sensitized solar cells (DSSCs) have attracted significant attention as a low-cost alternative to conventional solid-state photovoltaic devices [1–6]. The polypyridylruthenium complexes are the most successful charge-transfer sensitizers employed in these cells, with the highest solar-to-electric power conversion efficiencies over 12% [7] achieved under simulated sunlight. However, the main drawback of the ruthenium complex-based sensitizers is the lack of absorption in the red region of the visible spectrum [8], which limits the further increase of the efficiencies of this type of sensitizer. On the contrary, phthalocyanine (Pc) and metallophthalocyanine (MPc) exhibit comparatively high molar extinction coefficients of approximately $10^5\ cm^{-1}\ M^{-1}$ in the Q band lying at 650–700 nm and are considered very good near infrared sensitizers.

An unsymmetrical zinc phthalocyanine sensitizer PCH001 containing three tert-butyl and two carboxylic acid groups acting as "push" and "pull" groups was reported with a 75% maximum incident photon-to-current conversion efficiency (IPCE) and a 3.05% power conversion efficiency (η) under one-sun simulated solar irradiation when incorporated into a liquid electrolyte cell [9]. PCH003 has six butyloxy groups that act as electron donors, which further extends the "push–pull" concept [10]. However, due to the poor electron injection rate of PCH003, the IPCE of 25% and the power conversion efficiency of 1.13% were observed under one-sun simulated solar irradiation using a liquid electrolyte. Another unsymmetrical zinc phthalocyanine sensitizer TT1 with three tert-butyl groups and a carboxyl group linked directly to the Pc ring showed 80% IPCE at 690 nm and a record efficiency of 3.52% under one-sun [11]. The same group reported a series of new complexes derived from TT1 through modification of the anchoring ligand, namely TT6, TT7, TT8, TT15 and TT16, to further increase the efficiency of zinc-phthalocyanine based solar cells [12]. A power conversion efficiency of 3.96% was obtained for TT15, which set a new record for TT1-based DSSCs. The highest efficiency for DSSCs using ZnPc sensitizers reported to date is 4.6% [13] and was achieved by a DSSC based on the sensitizer PcS6, which was a ZnPc

* Corresponding author. Tel.: +86 635 8230680; fax: +86 635 8239121.
** Corresponding author.
E-mail addresses: zhangxianxi@lcu.edu.cn, xxzhang3@gmail.com (X. Zhang), mars_dark@hotmail.com (X. Pan).

1093-3263/$ – see front matter © 2011 Elsevier Inc. All rights reserved.
doi:10.1016/j.jmgm.2011.12.001

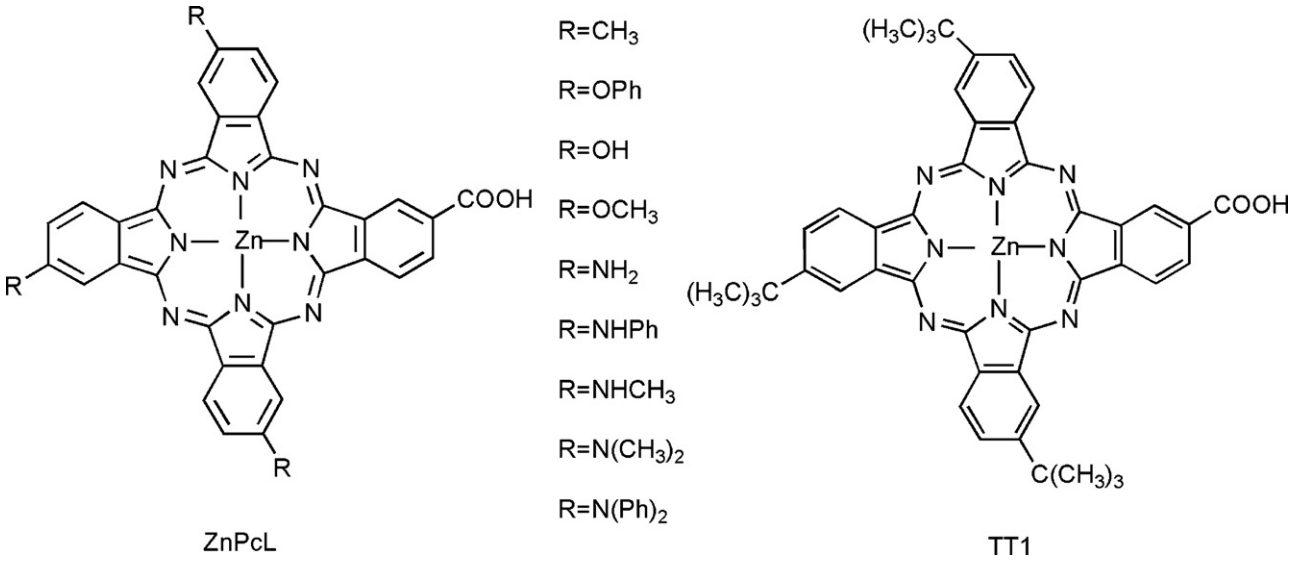

Fig. 1. The structures of the novel unsymmetrical ZnPcL and TT1.

complex with six 2,6-diphenylphenoxy groups and a phenylcarboxyl acid group [13]. The efficiencies of phthalocyanine-based DSSCs have increased rapidly in recent years; however, it is still necessary to further optimize the sensitizers to catch up with the ruthenium complex or porphyrin sensitizers.

There are still some factors that can influence the performances of phthalocyanine-based DSSCs. The energy matching between the lowest unoccupied molecular orbital (LUMO) of the sensitizers and the band edge of the semiconductor TiO_2 is one of the key factors that influence the electron injection of DSSCs. The LUMOs of the phthalocyanine sensitizers described above are generally too low to provide perfect electron injection, which should be further increased in the following optimizations. The lack of absorption in the 450–650 nm region is another limit to the performances of the phthalocyanine sensitizers, which results in them being considered only as near infrared sensitizers. The phthalocyanine complexes would be much more promising for developing panchromatic sensitizers and, thus, provide much higher efficiencies if new absorptions bands could be created in this region. Additionally, the peripheral substituents also play important roles in tuning the molecular orbital energy levels, increasing the solubility and reducing the aggregation of zinc phthalocyanine complexes used in DSSC [14–17]. These factors should be considered in further optimization of the phthalocyanine sensitizers.

In addition to experimental investigations, quantum chemistry calculations have also been used to interpret the structure–performance relationships and screen promising candidates of various sensitizers used in DSSCs. Filippo De Angelis and coworkers have conducted pioneering theoretical studies on the polypyridyl Ruthenium complexes and the diphenylamine-based sensitizers [8,18–21]. Cui and coworkers designed and screened a few new Pc sensitizer candidates derived from PCH001 and compared them with PCH001 as well as TT1 at the density functional B3LYP level using LANL2DZ and 3-21g* basis sets [22]. Wan and coworkers studied a series of unsymmetrical phthalocyaninato zinc complexes to control the directionality of the charge transfer at B3LYP level using LANL2DZ and 6-31G* basis sets [23]. Similar semi-empirical [24] and density functional [25–28] studies have also been used for the interpretation and screening of porphyrin sensitizers. Theoretical calculations are becoming an extremely powerful tool for the design and screening of novel sensitizer candidates, especially when associated with experimental synthetic efforts, which might eventually lead to new and more efficient products.

In this paper, nine new molecular structures were designed to find appropriate candidates for creating improved solar cells. The structures of the sensitizers ZnPcL–R (R = —CH_3, —OH, —OCH_3, —OPh, —NH_2, —$NHCH_3$, —$N(CH_3)_2$, —NHPh and —$N(Ph)_2$) and TT1 are shown in Fig. 1, comparatively. A carboxyl group is directly attached to the phthalocyanine ring serving as the anchoring group. The groups ranging from —CH_3, —OH, —OCH_3, —OPh, —NH_2, —$NHCH_3$, —$N(CH_3)_2$ and —NHPh to —$N(Ph)_2$ were linked to the phthalocyanine ring replacing the tert-butyl groups of TT1 to further enhance electron-donating ability and solubility.

Density functional calculations using the B3LYP functional with the LANL2DZ basis set were performed to predict the orbital energy levels and the electronic absorption spectra of the novel unsymmetrical zinc phthalocyanine complexes comparatively with those of TT1. The molecular orbital spatial orientations of the ZnPcL series molecules and TT1 are also discussed to explain the discrepancy of the electron-separation abilities. Promising candidate complexes that may be used for developing more efficient DSSCs were screened by comparing these new molecules to the TT1 dye with a known solar cell efficiency of 3.52% under one-sun simulated solar irradiation [11]. The novel candidates bearing the —NH_2, —$NHCH_3$, —$N(CH_3)_2$, —NHPh and —$N(Ph)_2$ moieties as donors were found to be very promising for providing superior performances to TT1 or even the current 4.6% efficiency record holder, PcS6. They were found to have higher LUMO levels, smaller energy gaps and red-shifted absorption bands. The new absorption bands emerging in the 450–650 nm region may promote ZnPcL—NH_2, ZnPcL—$NHCH_3$, ZnPcL—$N(CH_3)_2$, ZnPcL—NHPh and ZnPcL—$N(Ph)_2$ from near infrared to panchromatic sensitizers. Further experimental synthetic efforts are in progress in our group to validate the predictions in this report.

2. Computational methods

Two basic functions of the theoretical computation are (i) to interpret the experimental results; and (ii) to predict properties of unknown molecules or materials, which is very useful for the design and screening of better molecules and materials. High accuracy and complicated models are much preferred to computation efficiency for interpretation of the experimental data, in which a few samples can be computed over a long time with well-equipped computers.

Table 1
Selected lowest-excited energies (ΔE), absorption wavelengths, oscillator strengths (f) and domination excitation characters for a low-lying singlet state of TT1 in ethanol.

State	Main configuration	ΔE, eV (λ, nm)	F	Excitation character	Exp. ΔE[e] (eV)
1	197[a] to >198[b] 62%	1.92 (645)	0.648	π–π*[c]	1.82
2	197 to >199 62%	2.02 (615)	0.596	π–π*	1.86
9	194 to >198 57%	3.20 (388)	0.198	LMCT[d]	
14	190 to >198 48%	3.43 (361)	0.326	π–π*	
16	190 to >198 35%	3.48 (356)	0.317	π–π*	
18	189 to >198 40%	3.55 (349)	0.468	π–π*	3.54
19	190 to >199 49%	3.57 (347)	0.427	π–π*	

[a] HOMO.
[b] LUMO.
[c] π–π*, excitation from π to π* orbital.
[d] LMCT, ligand to metal charge transfer.
[e] Ref. [11].

However, for the design and screening of better molecules and materials in which large quantities of samples are required to be computed in a relatively short time, computation efficiency is much preferred to high accuracy and complex models. As long as qualitative variation trends of the properties of the samples can be obtained to screen promising candidates, ab initio, semi-empirical or even molecular mechanics calculations may be used. Balancing the accuracy and the computation cost, density functional theory (DFT) and time-dependent density functional theory (TDDFT) calculations that were successfully used in previous research were adopted in this study.

Several models are available regarding the electron injection process from the sensitizers to the semiconductor electrode. A widely used, simple model considers the LUMO level of the sensitizer and the conduction band edge of the semiconductor [8,18,19,22–28]. Another precise and more complicated model considers the excited state oxidation potential, which involves the combination of the ground state oxidation potential at various levels of approximations and of the lowest dye excited state possibly involving relaxation of the dye excited state geometry [20,21]. An even more complicated model should also consider the surface heterogeneity of the metal oxide, different sensitizer anchoring modes and the injection from a variety of different excited states (i.e., singlet, triplet, etc.). After assessing the accuracy and efficiency of using each of these models, the first simple model was adopted in this study.

Full geometric optimizations of the novel unsymmetrical ZnPcL sensitizers and TT1 were performed using the B3LYP exchange-correlation functional [29] and a LANL2DZ basis set. The Berny algorithm using redundant internal coordinates [30] was employed in energy minimization and the default cutoffs were used throughout. Vibrational frequency calculations were conducted to be certain that the optimized structures were true energy minima. None of the frequency calculations generated imaginary frequencies, indicating that true energy minima were really achieved. Natural bond orbital analysis was carried out on the basis of the minimized structure with NBO 3.1 embedded in the Gaussian03 program [31]. The electronic excitation states of the above sensitizers were calculated with TDDFT at B3LYP level with the LANL2DZ basis set in ethanol, and the TDDFT calculations were conducted using non-equilibrated solvent conditions with PCM model. Corresponding electronic absorption spectra were simulated by fitting to the Lorentzian line shape with a half-width at half-maximum of 8 nm. Mizuseki et al. [32] suggested that the charge transport was also related to the spatial distributions and the compositions of the frontier molecular orbitals. Thus, the compositions and

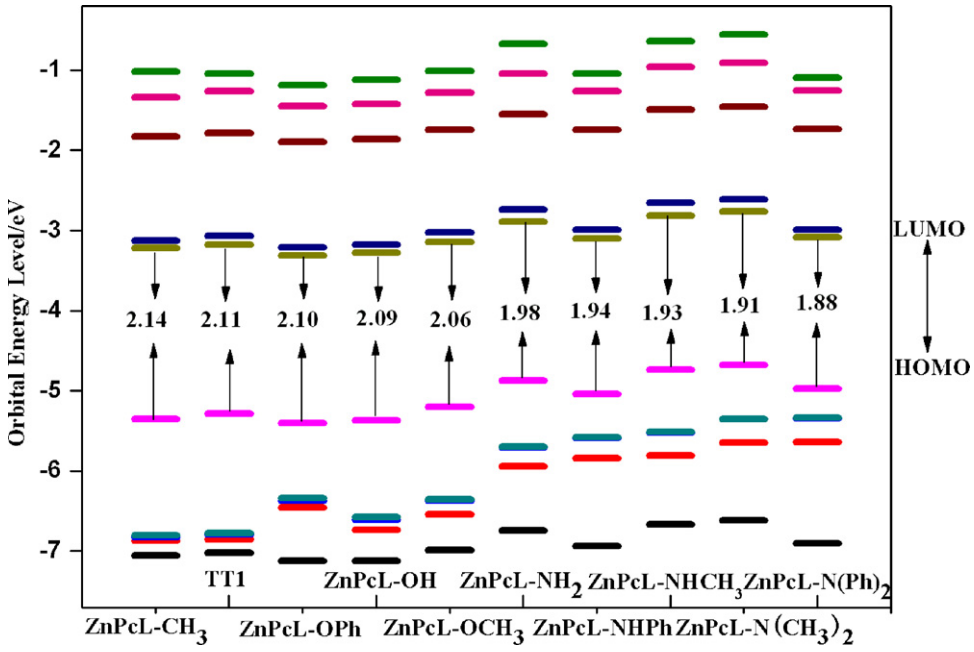

Fig. 2. Molecular orbital energy levels of ZnPcL—CH_3, TT1, ZnPcL—OPh, ZnPcL—OH, ZnPcL—OCH_3, ZnPcL—NH_2, ZnPcL—NHPh, ZnPcL—$NHCH_3$, ZnPcL—$N(CH_3)_2$ and ZnPcL—$N(Ph)_2$.

Table 2
Orbital energy levels of the ZnPcL series molecules and TT1.

Molecule	ε_{HOMO}	$\Delta\varepsilon_{LUMO-HOMO}$	ε_{LUMO}
ZnPcL—OPh	−5.40	2.10	−3.31
ZnPcL—OH	−5.37	2.09	−3.28
ZnPcL—CH_3	−5.36	2.14	−3.22
TT1	−5.28	2.11	−3.17
ZnPcL—OCH_3	−5.20	2.06	−3.15
ZnPcL—NHPh	−5.04	1.94	−3.10
ZnPcL—$N(Ph)_2$	−4.97	1.88	−3.09
ZnPcL—NH_2	−4.87	1.98	−2.89
ZnPcL—$NHCH_3$	−4.74	1.93	−2.81
ZnPcL—$N(CH_3)_2$	−4.68	1.91	−2.76

spatial distributions of the HOMO and LUMO of these molecules were also calculated to obtain more information. All calculations were performed on an IBM P690 system in the Shandong Province High Performance Computer Center.

3. Results and discussion

3.1. Comparison of the theoretical and experimental spectra of TT1

The corresponding theoretical and experimental lowest-excited energies (ΔE) of TT1 are listed in Table 1. The experimental spectrum of TT1 shows three main features, which are well reflected in the spectrum simulated. Two, almost equally intense bands are located at 1.82 and 1.86 eV. The intense band at the higher energy region is located at 3.54 eV [11]. The theoretical spectrum of TT1 also shows three main features. Two, almost equally intense bands are located at 1.92 and 2.02 eV. The intense band at the higher energy region is located at 3.55 eV. The agreement between theory and experiment is good, indicating that the calculation method using B3LYP functional combined with the LANL2DZ basis set is appropriate for such types of molecules.

3.2. The electronic structure of the ground state

The molecular orbital energy levels of these complexes are shown in Fig. 2 according to the energy gaps between HOMO and LUMO, from large to small. The energy levels of ten molecular orbitals ranging from HOMO−4 to LUMO+4 of the ZnPcL molecules (A–I) and TT1 are displayed in the figure. The corresponding data of HOMO, LUMO and HOMO–LUMO gaps are listed in Table 2 according to the LUMO from high to low. The influences of different substituents on the molecular orbital energy levels can be obtained from this figure and table.

The HOMO–LUMO gaps of the dye molecules have a close relationship to the absorption band positions of the sensitizers. The smaller energy gaps make the electrons more easily to be excited and are thus a benefit for absorbing the longer-wavelength light. Hence, more photons can be absorbed at the same time, which may contribute to obtaining a higher short circuit current density J_{sc} and overall power conversion efficiency η. As observed in Fig. 2, the frontier molecular orbital energy gaps are significantly affected by those different peripheral substituents attached to the phthalocyanine ring. The smallest energy gap between HOMO and LUMO is 1.88 eV for ZnPcL—$N(Ph)_2$ among all the phthalocyanine derivatives in this study. However, ZnPcL—CH_3 has the largest energy gap of 2.14 eV among these sensitizer candidates. Most of the novel sensitizer candidates have smaller HOMO–LUMO gaps than that of TT1, showing that most also show potential for providing red-shifted electronic absorption spectra compared to TT1. The molecular orbital energy gaps reduce gradually along the variation of the peripheral substituents whose electron-donating abilities are increased, which shows that powerful electron-donating substituents are very helpful in moving the absorption bands to the longer wavelength side.

The LUMO level of the sensitizer has a close relationship with the electron injection efficiency of the TiO_2 surface. A higher LUMO level is helpful for providing higher electron injection potential and, thus, higher electron injection efficiency and higher energy conversion efficiency η. The phthalocyanine sensitizers reported previously, including TT1, generally have too low LUMO levels as matched with the conduction band of TiO_2, which limits the further improvement of the energy conversion efficiency of phthalocyanine-sensitized solar cells. Thus, it is very important to screen novel phthalocyanine sensitizer candidates with a higher LUMO level than that of TT1. As observed in Table 2, the novel sensitizer candidates with the methoxyl substituent and all the amino-derived substituents have higher LUMO energy levels than that of TT1, showing that these candidates are promising for providing higher electron injection efficiencies than those of TT1. Comparing these different substituents, it was observed that the candidates with amino-derived substituents had higher LUMO levels than those with hydroxyl-derived substituents. The candidates with alkyl groups in the substituents had even higher LUMO levels than those with aryl groups in the substituents. These observed trends may provide valuable information for the further tuning of the LUMO levels in new sensitizer designs.

Besides the LUMO level, the HOMO level of the sensitizer is also very important for the functioning of DSSC, especially for the dye-regeneration process. Because the theoretical redox potential of the electrolyte is difficult to be obtained, another reference is necessary for assessing the sensitizer candidates. N3 dye, the best dye from the ruthenium–polypyridyl sensitizer family, is a good choice as the reference. The sensitizer candidates with HOMO level close to that of the N3 dye would be promising for the regeneration since the N3 dye can be regenerated very well.

The highest one among the HOMOs of all the ZnPcL molecules is −4.68 eV, while the HOMO of N3 is −5.08 eV calculated with the same method, meaning that the highest HOMO level of ZnPcL is 0.4 eV higher than that of N3. The driving force for regeneration of N3 is 0.75 eV [6], indicating that the driving forces for the ZnPcL sensitizer candidates are still more than 0.35 eV. Wenger and coworkers [33] reported recently that the sensitizers with a small driving force as little as 0.15 eV could operate functionally in DSSCs, which eventually aided in reducing the photovoltage losses due to poor energetic alignment of the materials. According to this literature, the HOMO levels of the ZnPcL sensitizer candidates studied in this work are still low enough for the regeneration process.

3.3. The molecular orbital spatial distribution

Mizuseki and coworkers [32] suggested that the charge transport was also related to the spatial distribution and the composition of the frontier orbital. To obtain more information about the molecules, the spatial distribution and the composition of the HOMO and LUMO for TT1 and the ZnPcL series molecules were also calculated. The graphs and the data of these results are shown in Fig. 3 and Table 3, respectively.

As observed in Fig. 3, the HOMOs of the ZnPcL series molecules and TT1 are mainly localized at the central phthalocyanine ring and the three electron-donating substituents, while the LUMOs are much more aligned with the carboxyl group, which indicates good electron-separated states. The photoexcited electrons would transfer from the phthalocyanine skeleton to the carboxyl group during the excitation process, which is a benefit to the injection of the photoexcited electrons to the conduction band of the semiconductor.

The contribution of the electron donating groups (—CH_3, —OH, etc.) and the electron accepting group (—COOH) to the compositions

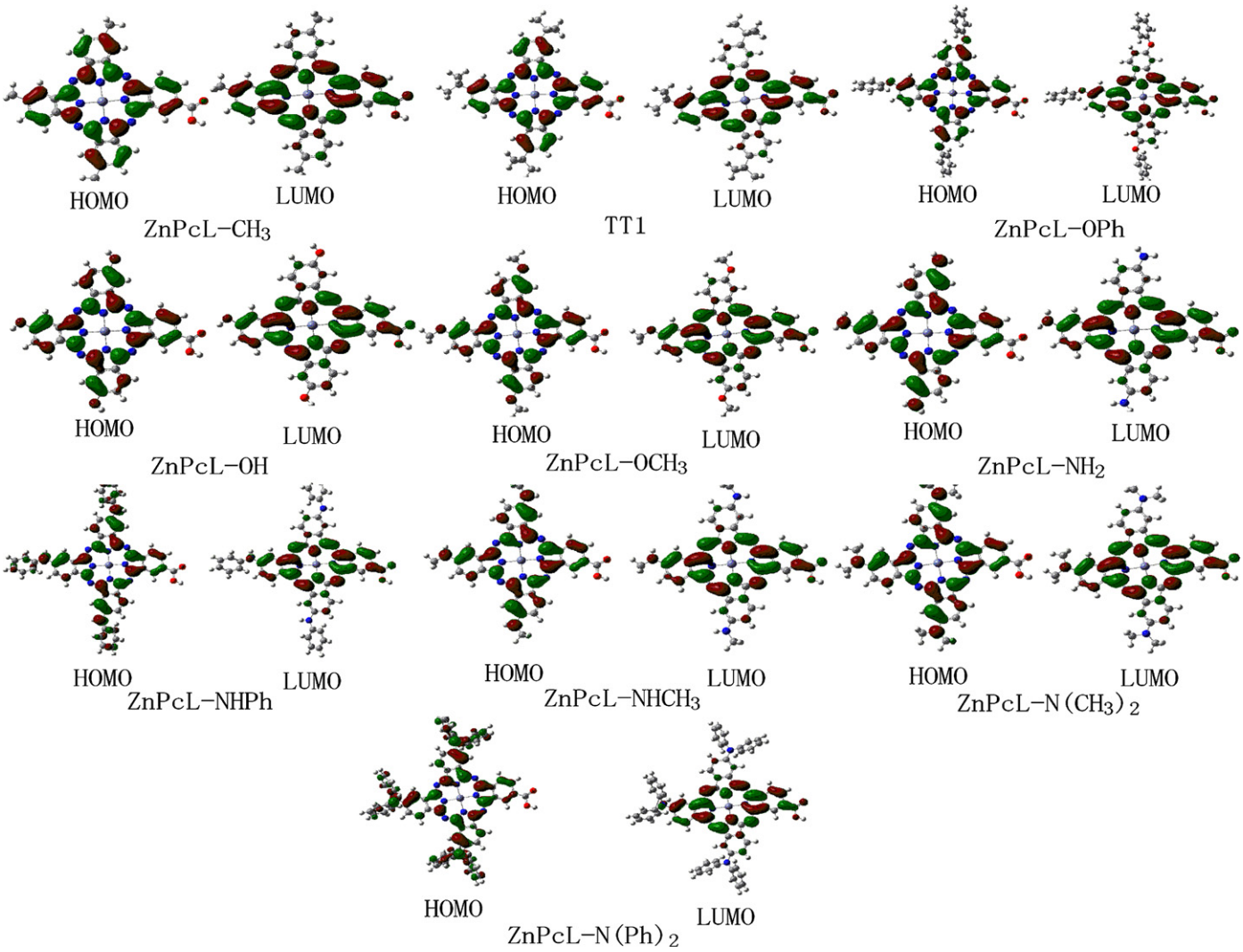

Fig. 3. Molecular orbital distributions of ZnPcL—CH_3, TT1, ZnPcL—OPh, ZnPcL—OH, ZnPcL—OCH_3, ZnPcL—NH_2, ZnPcL—NHPh, ZnPcL—$NHCH_3$, ZnPcL—$N(CH_3)_2$ and ZnPcL—$N(Ph)_2$.

of HOMO and LUMO for all the compounds were calculated and listed in Table 3. The compositions of the electron donating groups for all the sensitizers are the average compositions of the three groups attached to the phthalocyanine ring.

As observed from Table 3, the contributions of the carboxyl groups to the LUMOs are much larger than those to the HOMOs for each compound, while the contributions of the electron-donating substituents to the LUMOs are much smaller than those to the HOMOs for each compound. This shows that the HOMOs are located primarily at the donor parts, while the LUMOs are more located at the acceptor parts, which agrees well with the molecular orbital spatial distribution shown in Fig. 3.

The compositions of the HOMOs of the electron donors for ZnPcL—CH_3, ZnPcL—OH and ZnPcL—NH_2 increase gradually, which implies that the electron-donating abilities are related to the atoms directly linked to the phthalocyanine rings. The composition of the donor moieties containing a nitrogen atom among the three donor groups is the largest. When the donor moieties have the same bridging atom, the compositions of the HOMO and LUMO of these groups have a close relationship with the species and number of the substituents on the bridging atom. In other words, the stronger the electron-donating abilities of the donor groups are, the larger compositions of these groups would be possessed in the HOMOs.

The contribution of the electron donating groups to the of the HOMOs of ZnPcL—NHPh and ZnPcL—$N(Ph)_2$ are the largest, which is because the number of atoms of their donor groups is the largest. The significant decreases of their contributions to the LUMOs are also observed, which agree well with the variation trends described above.

In sum, the compositions of these donor groups possessing corresponding phthalocyanine molecules are related to the electron-donating abilities of the donor moieties, the bridging atoms between the phthalocyanine ring and the donor group as well as the number of atoms that the donor groups have.

3.4. Electronic absorption spectra

The lowest 40 singlet–singlet excitations of the nine complexes and TT1 were calculated in ethanol to gain further insight into the excited states of the candidates using TDDFT calculations. The theoretical absorption spectra data are listed in Table 4. The electronic absorption spectra were simulated by fitting to the Lorentzian line shape with a half-width at half-maximum of 8 nm as shown in Fig. 4.

All the zinc phthalocyanine complexes except ZnPcL—CH_3 have more absorption bands than TT1 at the longer-wavelength side as shown in Fig. 4. The comparison between the compounds

Table 3
Molecular orbital compositions of the ZnPcL series molecules and TT1 (%).

Molecule	Group	HOMO	LUMO
ZnPcL—CH_3	—COOH	0.48	2.21
	—CH_3	0.29	0.13
TT1	—COOH	0.49	2.09
	—$C(CH_3)_3$	0.53	0.34
ZnPcL—OPh	—COOH	0.45	2.07
	—OPh	2.21	0.49
ZnPcL—OH	—COOH	0.47	2.09
	—OH	1.45	0.28
ZnPcL—OCH_3	—COOH	0.48	2.18
	—OCH_3	2.14	0.39
ZnPcL—NH_2	—COOH	0.50	2.67
	—NH_2	3.74	0.52
ZnPcL—NHPh	—COOH	0.39	2.33
	—NHPh	8.04	0.90
ZnPcL—$N(CH_3)_2$	—COOH	0.47	2.61
	—$N(CH_3)_2$	6.76	0.82
ZnPcL—$N(Ph)_2$	—COOH	0.31	2.33
	—$N(Ph)_2$	12.7	1.06

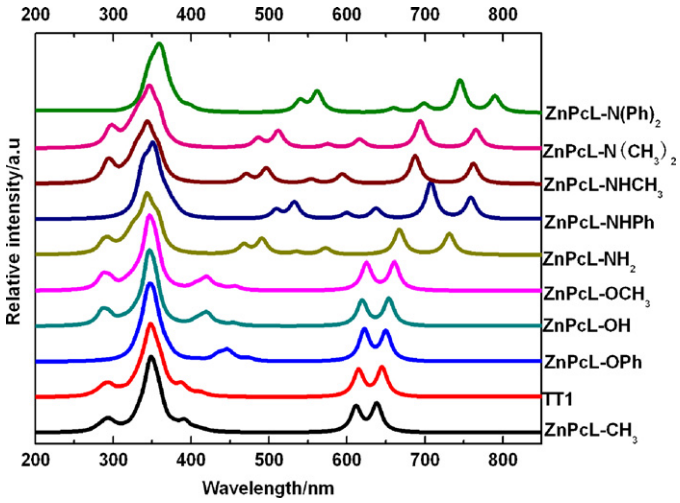

Fig. 4. Electronic absorption spectra of ZnPcL—CH_3, TT1, ZnPcL—OPh, ZnPcL—OH, ZnPcL—OCH_3, ZnPcL—NH_2, ZnPcL—NHPh, ZnPcL—$NHCH_3$, ZnPcL—$N(CH_3)_2$ and ZnPcL—$N(Ph)_2$.

ZnPcL—CH_3 and TT1 shows that they almost have the same profiles in the electronic absorption spectra. Similarly, ZnPcL—OPh, ZnPcL—OH and ZnPcL—OCH_3 have the same profiles. ZnPcL—NH_2, ZnPcL—NHPh, ZnPcL—$NHCH_3$, ZnPcL—$N(CH_3)_2$ and ZnPcL—$N(Ph)_2$ show another similar profile. The difference is that the later has a slightly bathochromic shift to the former, which corresponds well with the electron-donating effect of the additional donor groups. The figures of all the compounds imply that the positions of the electronic absorption spectra may be mainly dependent on the atoms that are directly connected to the phthalocyanine rings.

The absorption bands of ZnPcL—$N(Ph)_2$ are mostly red-shifted among these compounds, which corresponds well with its smallest HOMO–LUMO gap. The longest absorption wavelengths calculated for ZnPcL—NH_2, ZnPcL—NHPh, ZnPcL—$NHCH_3$, ZnPcL—$N(CH_3)_2$ and ZnPcL—$N(Ph)_2$ red shift largely with respect to that of TT1. The bands found at 732, 759, 763, 767 and 790 nm for ZnPcL—NH_2, ZnPcL—NHPh, ZnPcL—$NHCH_3$, ZnPcL—$N(CH_3)_2$ and ZnPcL—$N(Ph)_2$ in the calculated spectra are 87, 114, 118, 122 and 145 nm red-shifted with respect to that of TT1 at 645 nm, respectively. This is partly contributed from the narrower orbital energy gaps, which are consistent with the variation trend of the absorption bands. Longer wavelength light can thus be absorbed and contribute to providing a larger short circuit current J_{sc} and, thus, higher photon-to-current conversion efficiency η.

Because the experimental ΔE of TT1 is even lower than its theoretical ΔE, it could be anticipated that the other complexes discussed above may provide even better performances than the theoretical prediction.

It is very interesting to note that several small absorption bands emerge in the spectra of the complexes that contain amino or amino-derived groups as donors in the 450–650 nm regions, which correspond to the blank region from 450 to 600 nm for TT1. It is well known in this field that phthalocyanine sensitizers have strong absorptions in the 650–700 nm regions, which makes them very useful as near infrared sensitizers. However, the lack of absorption between 450 and 650 nm signifies a great waste of photons in this region, which significantly limits a further increase of the overall power conversion efficiencies of phthalocyanine-sensitized solar cells. If the new absorption bands theoretically predicted in this region could be finally confirmed, benchmark progress that promotes phthalocyanine dyes from near infrared sensitizers to panchromatic sensitizers could be achieved.

Some significant excitations in this region for these compounds are listed in Table 4 and corresponding molecular orbital distributions are shown in Fig. 5. The reason why these new peaks emerge in the 450–650 nm regions can be expounded as follows

Table 4
Selected lowest-excited energies (ΔE), absorption wavelengths, oscillator strengths (f) and domination excitation characters for a low-lying singlet state of ZnPcL—NH_2, ZnPcL—NHPh, ZnPcL—$NHCH_3$, ZnPcL—$N(CH_3)_2$ and ZnPcL—$N(Ph)_2$.

State	Main configuration	ΔE, eV (λ, nm)	F	State	Main configuration	ΔE, eV (λ, nm)	f
	ZnPcL—NH_2				ZnPcL—NHPh		
3	160[a] > 162[b] 58%	2.16 (574)	0.095	3	220[a] to >222[b] 52%	1.94 (638)	0.131
4	159 to >162 58%	2.17 (572)	0.055	4	219 to >222 53%	1.95 (637)	0.105
5	160 to >163 66%	2.31 (536)	0.055	5	220 to >223 67%	2.07 (600)	0.125
7	158 to >162 65%	2.52 (491)	0.345	7	218 to >222 66%	2.33 (533)	0.370
8	158 to >163 65%	2.65 (468)	0.208	8	218 to >223 66%	2.43 (509)	0.192
	ZnPcL—$NHCH_3$				ZnPcL—$N(CH_3)_2$		
3	171 to >174 65%	2.07 (600)	0.025	3	183 to >186 66%	1.99 (622)	0.022
4	172[a] to >174[b] 64%	2.09 (594)	0.196	4	184[a] to >186[b] 64%	2.01 (616)	0.186
5	172 to >175 67%	2.24 (554)	0.094	5	184 to >187 67%	2.01 (616)	0.085
7	170 to >174 66%	2.50 (497)	0.341	7	182 to >186 65%	2.50 (497)	0.383
8	170 to >175 60%	2.63 (471)	0.192	8	182 to >187 65%	2.63 (471)	0.211
	ZnPcL—$N(Ph)_2$						
3	280[a] to >282[b] 62%	1.77 (700)	0.154	7	278 to >282 65%	2.21 (562)	0.469
4	279 to >282 62%	1.78 (697)	0.038	8	278 to >283 65%	2.30 (540)	0.261
5	280 to >283 68%	1.88 (660)	0.095				

[a] HOMO−1.
[b] LUMO.

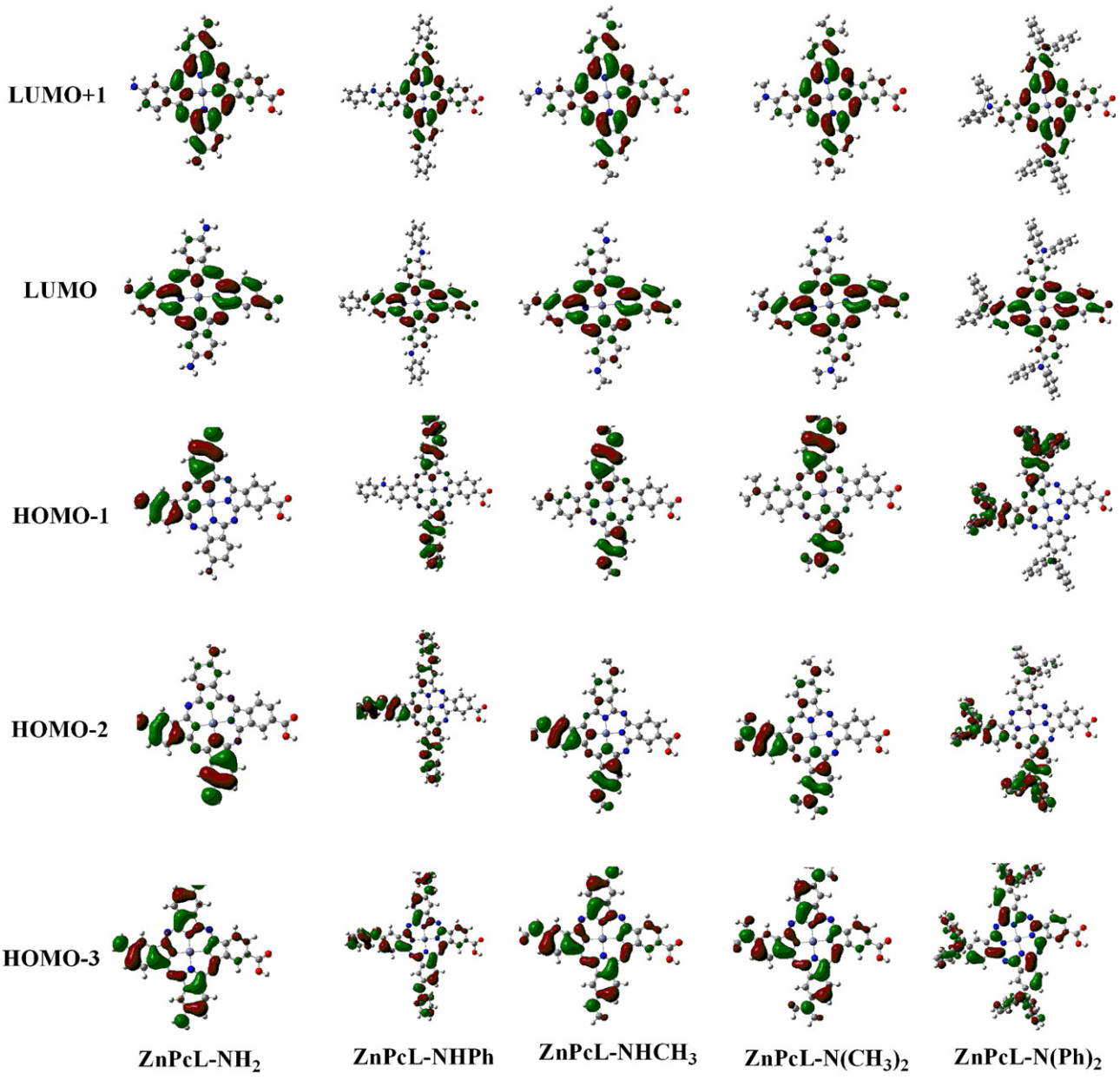

Fig. 5. Molecular orbital distribution for ZnPcL—NH_2, ZnPcL—NHPh, ZnPcL—$NHCH_3$, ZnPcL—$N(CH_3)_2$ and ZnPcL—$(Ph)_2$.

according to the data in the table and the molecular orbital distribution in the figure.

As shown in Table 4, the new absorption bands emerging in the range of 450–650 nm mainly originate from the transitions from HOMO−3 to LUMO+1 or HOMO-3 and HOMO−1 to LUMO. The spatial distributions of HOMO−3 and HOMO−1 were mainly located at the donor moieties, including significant contributions from the peripheral substituents, whereas the distributions of LUMO and LUMO+1 were principally located in the acceptor moieties and the phthalocyanine rings. The channel of the electron transfer and the formation of the absorption bands were well interpreted through the data listed in Table 4 and the orbital distributions shown in Fig. 5.

However, why these absorption bands could not emerge in this region in the spectra of TT1 and the other sensitizer candidate with hydroxyl-derived substituents can be interpreted from the molecular orbital energy levels shown in Fig. 2. Their energy levels of HOMO−3 to HOMO−1 are much lower than those of the molecules with the nitrogen bridging substituents, which move the absorptions to the shorter wavelength side appearing as shoulder bands near 400 nm as shown in Fig. 4.

It was also observed that molecules with the same bridging atoms between the phthalocyanine ring and the substituents had similar energy levels, while those with different bridging atoms and similar substituents had large differences in the energy levels for these molecular orbitals. This indicates that the bridging atoms between the phthalocyanine ring and the substituents are very important in tuning the molecular orbital energy levels and the electronic absorption spectra.

The absorption wavelength for ZnPc—$NHCH_3$ and ZnPcL—$N(CH_3)_2$ red-shifted a small degree compared to that of ZnPcL—NH_2, while the ZnPcL—NHPh and ZnPcL—$N(Ph)_2$ red-shifted significantly with respect to that of ZnPcL—NH_2. The result indicates that the electron-donating ability of the phenyl group is stronger than that of the methyl group. This evidence is also very helpful for the further design of better phthalocyanine sensitizers.

For the current record holder PcS6, which has six 2,6-diphenylphenoxy groups at the peripheral positions, there is still no absorption band observed in the 450–650 nm regions in its electronic absorption spectrum [13]. This agrees well with the conclusion drawn above that the bridging oxygen atom cannot bring new absorption bands in this region. That is to say, the contribution of the six 2,6-diphenylphenoxy groups are not generating new absorptions bands, but mainly are limited to preventing aggregation. Because the record efficiency of PcS6 had already reached 4.6%, the sensitizer candidates screened with new absorption bands in the 450–650 nm regions in this work and their further optimized designs are very promising for providing even higher efficiencies.

4. Conclusions

We present here density functional theory and time dependent density functional theory calculations of the novel sensitizer candidates formed by $-CH_3$, $-OH$, $-OCH_3$, $-OPh$, $-NH_2$, $-NHCH_3$, $-N(CH_3)_2$, $-NHPh$ and $-N(Ph)_2$ substituted phthalocyanine donors and carboxyl acceptor. Through the comparison between the nine novel unsymmetrical zinc phthalocyanine and TT1, as well as the current record holder PcS6, it is shown that the sensitizer candidates with nitrogen bridging substituents, namely ZnPcL$-NH_2$, ZnPcL$-NHCH_3$, ZnPcL$-N(CH_3)_2$, ZnPcL$-NHPh$ and ZnPcL$-N(Ph)_2$, are very promising for providing higher efficiencies than that of TT1 or even the current 4.6% efficiency record of PcS6. They have higher LUMO levels, smaller energy gaps and red-shifted absorption bands. The new absorption bands that emerged in the 450–650 nm region may promote ZnPcL$-NH_2$, ZnPcL$-NHCH_3$, ZnPcL$-N(CH_3)_2$, ZnPcL$-NHPh$ and ZnPcL$-N(Ph)_2$ from near infrared to panchromatic sensitizers.

Although illustrative discussions and predictions are provided in this context, the authors still insist that they should only be considered as qualitative rather than quantitative proof in further sensitizer design because of the limited accuracy of the calculation methods available for such large molecules. Further experimental synthetic efforts are underway in our group to validate the predictions in this report.

This work is valuable not only for the theoretical chemists who work on the structure-property relationships between the sensitizers and corresponding solar cells, but also for the experimental chemists who work on developing novel sensitizers with higher energy conversion performances.

Acknowledgments

The authors thank the National Basic Research Program of China (Grant No. 2011CBA00701, 2010CB234601), the National High Technology Research and Development Program of China (Grant No. 2011AA050510), the National Natural Science Foundation of China (Grant No. 21171084), the Returned Overseas Researcher Foundation from the Ministry of Education, the Tai-Shan Scholar Research Fund and the Key Lab of Novel Thin Film Solar Cells (KF200904), CAS, for financial support.

References

[1] M. Grätzel, Photoelectrochemical cells, Nature 414 (2001) 338–344.
[2] M. Grätzel, Dye-sensitized solar cells, J. Photochem. Photobiol. C 4 (2003) 145–153.
[3] Md.K. Nazeeruddin, Michael Grätzel Festschrift, attribute for his 60th birthdays, Coord. Chem. Rev. 248 (2004) 1161–1164.
[4] N. Robertson, Optimizing dyes for dye-sensitized solar cells, Angew. Chem. Int. Ed. 45 (2006) 2338–2345.
[5] T.W. Hamann, R.A. Jensen, A.B.F. Martinson, H.V. Ryswyk, J.T. Hupp, Advancing beyond current generation dye-sensitized solar cells, Energy Environ. Sci. 1 (2008) 66–78.
[6] A. Hagfeldt, G. Boschloo, L. Sun, L. Kloo, H. Pettersson, Dye-sensitized solar cells, Chem. Rev. 110 (2010) 6595–6663.
[7] M. Grätzel 3rd, Dye Solar Cell Industrialization Conference, April 22–24, Nara, Japan, 2009.
[8] M.K. Nazeeruddin, F.D. Angelis, S.A. Fantacci, G. Selloni, P. Viscardi, S. Liska, B. Ito, M. Takeru, Grätzel, Combined experimental and DFT-TDDFT computational study of photoelectrochemical cell ruthenium sensitizers, J. Am. Chem. Soc. 127 (2005) 16835–16847.
[9] P.Y. Reddy, L. Giribabu, C. Lyness, H.J. Snaith, C. Vijaykumar, M. Chandrasekharam, M. Lakshmikantam, J.H. Yum, K. Kalyanasundaram, M. Grätzel, M.K. Nazeeruddin, Efficient sensitization of nanocrystalline TiO_2 films by a near-IR-absorbing unsymmetrical zinc phthalocyanine, Angew. Chem. Int. Ed. 46 (2007) 373–376.
[10] L. Giribabu, C. Vijay Kumar, V. Gopalreddy, V. Gopal Reddy, P. Yella Reddy, C. Srinivasa Rao, S.R. Jang, J.H. Yum, M.K. Nazeeruddin, M. Grätzel, Unsymmetrical alkoxy zinc phthalocyanine for sensitization of nanocrystalline TiO_2 films, Sol. Energy Mater. Sol. Cells 91 (2007) 1611–1617.
[11] J.J. Cid, J.H. Yum, S.R. Jang, M.K. Nazeeruddin, E. Palomares, J. Ko, M. Grätzel, T. Torres, Molecular cosensitization for efficient panchromatic dye-sensitized solar cells, Angew. Chem. Int. Ed. 46 (2007) 8358–8362.
[12] M. García-Iglesias, J. Cid, J. Yum, A. Forneli, P. Vázquez, M.K. Nazeeruddin, E. Palomares, M. Grätzel, T. Torres, Increasing the efficiency of zinc-phthalocyanine based solar cells through modification of the anchoring ligand, Energy Environ. Sci. 4 (2011) 189–194.
[13] S. Mori, M. Nagata, Y. Nakahata, K. Yasuta, R. Goto, M. Kimura, M. Taya, Enhancement of incident photon-to-current conversion efficiency for phthalocyanine-sensitized solar Cells by 3D molecular structuralization, J. Am. Chem. Soc. 132 (2010) 4054–4055.
[14] N.B. McKeown, Phthalocyanine Materials: Synthesis, Structure and Function, Cambridge University Press, Cambridge, 1998, pp. 1–183.
[15] E.A. Lukyanets, V.N. Nemykin, The key role of peripheral substituents in the chemistry of phthalocyanines and their analogs, J. Porphyrins Phthalocyanines 14 (2010) 1.
[16] V.N. Nemykin, E.A. Lukyanets, in: K.K. Kadish, K.M. Smith, R. Guilard (Eds.), Handbook of Porphyrin Science, 3, World Scientific, Singapore, 2010, pp. 1–323.
[17] V.N. Nemykin, E.A. Lukyanets, Synthesis of substituted phthalocyanines, ARKIVOC 1 (2010) 136.
[18] F. De Angelis, S. Fantacci, A. Selloni, Md.K. Nazeeruddin, Time dependent density functional theory study of the absorption spectrum of the [Ru(4,4′-COO^-2,2′-bpy)2(X)2]4^- (X = NCS, Cl) dyes in water solution, Chem. Phys. Lett. 415 (2005) 115–120.
[19] F. De Angelis, S. Fantacci, A. Selloni, Md.K. Nazeeruddin, M. Grätzel, Time-dependent density functional theory investigations on the excited states of Ru(II)-dye-sensitized TiO_2 nanoparticles: The role of sensitizer protonation, J. Am. Chem. Soc. 129 (2007) 14156–14157.
[20] F. De Angelis, S. Fantacci, A. Selloni, Alignment of the dye's molecular levels with the TiO_2 band edges in dye-sensitized solar cells: a DFT-TDDFT study, Nanotechnology 19 (2008) 424002, 7 pp.
[21] M. Pastore, S. Fantacci, F. De Angelis, Ab initio determination of ground and excited state oxidation potentials of organic chromophores for dye-sensitized solar cells, J. Phys. Chem. C 114 (2010) 22742–22750.
[22] H. Cui, R. Ma, P. Guo, Q. Zeng, G. Liu, X. Zhang, Molecule design and screening of novel unsymmetrical zinc phthalocyanine sensitizers for dye-sensitized solar cells, J. Mol. Model. 16 (2010) 303–310.
[23] L. Wan, D. Qi, Y. Zhang, J. Jiang, Controlling the directionality of charge transfer in phthalocyaninato zinc sensitizer for a dye-sensitized solar cell: density functional theory studies, Phys. Chem. Chem. Phys. 13 (2011) 1639–1648.
[24] M.P. Balanay, C.V.P. Dipaling, S.H. Lee, D.H. Kim, K.H. Lee, AM1 molecular screening of novel porphyrin analogues as dye-sensitized solar cells, Sol. Energy Mater. Sol. Cells 91 (2007) 1775–1781.
[25] R. Ma, P. Guo, H. Cui, X. Zhang, M.K. Nazeeruddin, M. Grätzel, Substituent effect on the meso-substituted porphyrins: theoretical screening of sensitizer candidates for dye-sensitized solar cells, J. Phys. Chem. A 113 (2009) 10119–10124.
[26] R. Ma, P. Guo, L. Yang, L. Guo, X. Zhang, M.K. Nazeeruddin, M. Grätzel, Theoretical screening of $-NH_2-$, $-OH-$, $-CH_3-$, $-F-$, and $-SH$-substituted porphyrins as sensitizer candidates for dye-sensitized solar cells, J. Phys. Chem. A 114 (2010) 1973–1979.
[27] R. Ma, P. Guo, L. Yang, L. Guo, Q. Zeng, G. Liu, X. Zhang, A theoretical interpretation and screening of porphyrin sensitizer candidates with anticipated good photo-to-electric conversion performances for dye-sensitized solar cells, J. Mol. Struct. Theochem. 942 (2010) 131–136.
[28] V.N. Nemykin, R.G. Hadt, R.V. Belosludov, H. Mizuseki, Y. Kawazoe, Influence of molecular geometry, exchange-correlation functional, and solvent effects in the modeling of vertical excitation energies in phthalocyanines using time-dependent density functional theory (TDDFT) and polarized continuum model TDDFT methods: can modern computational chemistry methods explain experimental controversies? J. Phys. Chem. A 111 (2007) 12901.
[29] A.D. Becke, Density-functional thermochemistry. III. The role of exact exchange, J. Chem. Phys. 98 (1993) 5648.
[30] C. Peng, P.Y. Ayala, H.B. Schlegel, M.J. Frisch, Using redundant internal coordinates to optimize equilibrium geometries and transition states, J. Comput. Chem. 17 (1996) 49.

[31] M.J. Frisch, G.W. Trucks, H.B. Schlegel, G.E. Scuseria, M.A. Robb, J.R. Cheeseman, J.A. Montgomery Jr., T. Vreven, K.N. Kudin, J.C. Burant, J.M. Millam, S.S. Iyengar, J. Tomasi, V. Barone, B. Mennucci, M. Cossi, G. Scalmani, N. Rega, G.A. Petersson, H. Nakatsuji, M. Hada, M. Ehara, K. Toyota, R. Fukuda, J. Hasegawa, M. Ishida, T. Nakajima, Y. Honda, O. Kitao, H. Nakai, M. Klene, X. Li, J.E. Knox, H.P. Hratchian, J.B. Cross, C. Adamo, J. Jaramillo, R. Gomperts, R.E. Stratmann, O. Yazyev, A.J. Austin, R. Cammi, C. Pomelli, J.W. Ochterski, P.Y. Ayala, K. Morokuma, G.A. Voth, P. Salvador, J.J. Dannenberg, V.G. Zakrzewski, S. Dapprich, A.D. Daniels, M.C. Strain, O. Farkas, D.K. Malick, A.D. Rabuck, K. Raghavachari, J.B. Foresman, J.V. Ortiz, Q. Cui, A.G. Baboul, S. Clifford, J. Cioslowski, B.B. Stefanov, G. Liu, A. Liashenko, P. Piskorz, I. Komaromi, R.L. Martin, D.J. Fox, T. Keith, M.A. Al-Laham, C.Y. Peng, A. Nanayakkara, M. Challacombe, P.M.W. Gill, B. Johnson, W. Chen, M.W. Wong, C. Gonzalez, J.A. Pople, Gaussian'03, revision B.05, Gaussian, Inc., Pittsburgh, PA, 2003.

[32] H. Mizuseki, K. Niimura, C. Majumder, R.V. Belosludov, A.A. Farajian, Y. Kawazoe, Theoretical study of donor–spacer–acceptor structure molecule for stable molecular rectifier, Mol. Cryst. Liq. Cryst. 406 (2003), 11/[205]–17/[211].

[33] S. Wenger, P.A. Bouit, Q. Chen, J. Teuscher, D. Di Censo, R. Humphry-Baker, J.E. Moser, J.L. Delgado, N. Martin, S.M. Zakeeruddin, M. Grätzel, Efficient Electron transfer and sensitizer regeneration in stable π-extended tetrathiafulvalene-sensitized solar cells, J. Am. Chem. Soc. 132 (2010) 5164–5169.